Anal. Chem. **2002,** *74,* 1136−1143

In-Channel Electrochemical Detection for Microchip Capillary Electrophoresis Using an Electrically Isolated Potentiostat

R. Scott Martin,[†] Kenneth L. Ratzlaff,[‡] Bryan H. Huynh,[†] and Susan M. Lunte*,[†]

Department of Pharmaceutical Chemistry and Center for Bioanalytical Research, The University of Kansas, 2095 Constant Avenue, Lawrence, Kansas 66047, and Instrumentation Design Laboratory, Department of Chemistry, The University of Kansas, Lawrence, Kansas 66045

A new electrode configuration for microchip capillary electrophoresis (CE) with electrochemical (EC) detection is described. This approach makes it possible to place the working electrode directly in the separation channel. The "in-channel" EC detection was accomplished without the use of a decoupler through the utilization of a specially designed, electrically isolated potentiostat. The effect of the working electrode position on the separation performance (in terms of plate height and peak skew) of poly(dimethylsiloxane)-based microchip CEEC devices was evaluated by comparing the more commonly used end-channel configuration with this new in-channel approach. Using catechol as the test analyte, it was found that in-channel EC detection decreased the total plate height by a factor of 4.6 and lowered the peak skew by a factor of 1.3. A similar trend was observed for the small, inorganic ion nitrite. Furthermore, a fluorescent and electrochemically active amino acid derivative was used to directly compare the separation performance of in-channel EC detection to that of a widely used laser-induced fluorescence (LIF) detection scheme. In this case, it was found that the plate height and peak skew for both detection schemes were essentially equal, and the separation performance of in-channel EC detection is comparable to LIF detection.

Over the past decade, utilization of the microchip format for capillary electrophoretic separations has witnessed extensive growth, from initial demonstrations[1−4] to high-throughput 96-channel DNA separations,[5] fully integrated multichannel separation-based immunoassays,[6] and complex two-dimensional separations.[7] Advantages to performing capillary electrophoresis (CE)-based separations in a microchip format are numerous and include fast analysis times, the use of high field strengths, minute consumption of solvents, and the possibility for disposable/portable devices.

Although detection in these devices has been accomplished by a variety of methods, including absorbance,[8] chemiluminescence,[9] electrochemiluminescence,[10] refractive index,[11] electrochemical,[12] conductimetry,[13−16] and Shah convolution Fourier transform detection,[17] by far the most widely utilized detection mode has been laser-induced fluorescence (LIF).[18] This is due primarily to the simplicity of constructing such systems, the ease of focusing a laser beam in the micrometer-sized channels, and the high performance of these detectors in terms of separation efficiencies and limits of detection.[19] There are a few drawbacks to LIF detection, however; these include the facts that only a small number of wavelengths can be used for excitation and pre- or postcolumn derivatization of the sample with a fluorophore is typically required.

Electrochemistry as a detection mode for microchip CE has received increased attention during the past five years and has recently been reviewed.[12,18] Electrochemical (EC) detection pro-

* Corresponding author. Phone: (785)-864-3811. Fax: (785)-864-5736. E-mail: slunte@ku.edu.

[†] Department of Pharmaceutical Chemistry and Center for Bioanalytical Research.

[‡] Instrumentation Design Laboratory.

(1) Harrison, D. J.; Manz, A.; Fan, Z.; Luedi, H.; Widmer, H. M. *Anal. Chem.* **1992**, *64*, 1926−1932.
(2) Effenhauser, C. S.; Manz, A.; Widmer, H. M. *Anal. Chem.* **1993**, *65*, 2637−2642.
(3) Jacobson, S. C.; Hergenroder, R.; Koutny, L. B.; Ramsey, J. M. *Anal. Chem.* **1994**, *66*, 1114−1118.
(4) Woolley, A. T.; Mathies, R. A. *Proc. Natl. Acad. Sci.* **1994**, *91*, 11348−11352.
(5) Shi, Y.; Simpson, P. C.; Scherer, J. R.; Wexler, D.; Skibola, C.; Smith, M. T.; Mathies, R. A. *Anal. Chem.* **1999**, *71*, 5354−5361.
(6) Cheng, S. B.; Skinner, C. D.; Taylor, J.; Attiya, S.; Lee, W. E.; Picelli, G.; Harrison, D. J. *Anal. Chem.* **2001**, *73*, 1472−1479.
(7) Gottschlich, N.; Jacobson, S. C.; Culbertson, C. T.; Ramsey, J. M. *Anal. Chem.* **2001**, *73*, 2669−2674.
(8) Salimi-Moosavi, H.; Jiang, Y.; Lester, L.; McKinnon, G.; Harrison, D. J. *Electrophoresis* **2000,** *21*, 1291−1299.
(9) Mangru, S. D.; Harrison, D. J. *Electrophoresis* **1998,** *19*, 2301−2307.
(10) Arora, A.; Eijkel, J. C. T.; Morf, W. E.; Manz, A. *Anal. Chem.* **2001,** *73*, 3282−3288.
(11) Swinney, K.; Markov, D.; Bornhop, D. J. *Anal. Chem.* **2000,** *72*, 2690−2695.
(12) Lacher, N. A.; Garrison, K. E.; Martin, R. S.; Lunte, S. M. *Electrophoresis* **2001,** *22*, 2526−2536.
(13) Liu, Y.; Wipf, D. O.; Henry, C. S. *Analyst* **2001**, *126*, 1248−1251.
(14) Kaniansky, D.; Masar, M.; Bielcikova, J.; Ivanyi, F.; Eisenbeiss, F.; Stanislawski, B.; Grass, A.; Neyer, A.; Johnck, M. *Anal. Chem.* **2000**, *72*, 3596−3604.
(15) Guijt, R. M.; Baltussen, E.; van der Steen, G.; Schasfoort, R. B. M.; Schlautmann, S.; Billiet, H. A. H.; Frank, J.; van Dedem, G. W. K.; van den Berg, A. *Electrophoresis* **2001**, *22*, 235−241.
(16) Lichtenberg, J.; Verpoorte, E.; de Rooij, N. F. In *Proceedings of Micro Total Analysis Systems 2001*; Ramsey, J. M., van den Berg, A., Eds.; Kluwer Academic Publishers: Dordrecht, The Netherlands, 2001, pp 323−324.
(17) Crabtree, H. J.; Kopp, M. U.; Manz, A. *Anal. Chem.* **1999**, *71*, 2130−2138.
(18) Schwarz, M. A.; Hauser, P. C. *Lab Chip* **2001**, *1*, 1−6.
(19) Orvick, G.; Tang, T.; Harrison, D. J. *Analyst* **1998**, *123*, 1429−1434.

10.1021/ac011087p CCC: $22.00
Published on Web 01/24/2002

vides many desirable features for a portable/disposable microchip system. Electrochemical detectors offer a high degree of selectivity and sensitivity while being amenable to miniaturization and relatively inexpensive to mass fabricate. Since the seminal papers from Ewing[20] and Mathies,[21] a number of other groups have described different variants of EC detection for microchip CE.[22−35] Although both conductimetry and potentiometry are widely used forms of electrochemical detection,[18] in this paper, use of the term electrochemical detection is made with reference to amperometric detection.

Despite the advantages of integrating EC detection with microchip CE, LIF remains the detection method of choice. This may be due in part to the inferior performance that EC detection has exhibited thus far in terms of the number of theoretical plates (N), peak shape, and sensitivity when compared to LIF detection. For example, to the best of our knowledge, the highest number of theoretical plates reported for microchip CEEC has been 21 000 for the neurotransmitter dopamine,[21] with typical limits of detection for microchip CEEC being in the mid-to-low-nanomolar range.[12] In addition, the peaks obtained with EC detection are typically unsymmetrical and exhibit tailing. Conversely, microchip CE-LIF normally results in symmetrical peaks and typical theoretical plate numbers in the hundreds of thousands. In a few cases, theoretical plate numbers approaching 1 000 000 have been demonstrated.[36,37] Detection limits using LIF detection are in the mid-to-low-picomolar range,[19] although these values are generally reported for fluorescent dyes. It is well-known that different chip substrates can lead to widely different separation efficiencies and peak shapes. Plastic and polymer devices, which are often used for microchip CEEC, usually yield less efficient separations than those fabricated from glass;[38] however, even considering this, the performance of EC detection for microchip CE is generally inferior.

One possible explanation for the poorer performance of EC detection for microchip CE is the design modifications that must be made to isolate the separation field from the EC detector. Although this isolation is necessary to diminish noise and protect the potentiostat, it can lead to extra-column effects. Commercially available potentiostats are grounded; if the working electrode is placed too close to the separation channel, the potentiostat provides a path to ground, exposing the detector electronics to the high separation fields. Except for two notable exceptions (explained below), this decoupling has normally been accomplished by aligning the working electrode in the detection reservoir, which is always grounded, in an end-channel configuration, tens of microns from the end of the separation channel. This is similar to the approach originally described for conventional CEEC.[39] Whereas LIF detects analytes *directly in* the separation channel, end-channel EC configurations detect analytes as they *exit* the separation channel. The distance between the working electrode and the end of the separation channel undoubtedly leads to band dispersion and loss of efficiency.

Two exceptions to the end-channel amperometric detection approach have been described, both of which use a decoupler to isolate the EC detector. Rossier and co-workers utilized a microchip device composed of two different polymers.[30] A decoupler was constructed by making several 10-μm holes in the top hydrophobic polyethylene layer. This allowed placement of the working electrode directly in the separation channel after the decoupler. In a separate study, Chen et al. used a palladium metal film decoupler in a Plexiglas-based microchip CEEC device.[31] Palladium is unique in its ability to absorb the hydrogen that is produced from the electrolysis of water at the electrophoretic ground. In this work, palladium metal was used for both the decoupler and working electrode. The working electrode was located in the separation channel 1 mm from the decoupler. In both of these studies, the number of theoretical plates and limits of detection were in the range of those quoted above for end-channel detection. No comparisons were made between the decoupler designs and the typical end-channel approach or LIF detection. Clearly, further studies are needed to fully evaluate the parameters that affect the separation performance of microchip CEEC.

In this paper, we describe a new electrode configuration that allows the working electrode to be placed directly in the separation channel without the use of a decoupler. This in-channel arrangement for EC detection is made possible by the development of a novel, electrically isolated potentiostat. This "floating" potentiostat was used to investigate the effect of the working electrode placement on the performance of microchip CEEC by comparing the typical end-channel alignment with this new in-channel approach in terms of plate height and the amount of peak tailing. Furthermore, a fluorescent and electrochemically active analyte was used to directly compare the in-channel approach for EC detection to the more widely used LIF detection scheme.

EXPERIMENTAL SECTION

Chemicals. The following chemicals and materials were used as received: SU-8 10 photoresist (MicroChem Corp., Newton, MA); propylene glycol methyl ether acetate and dodecyltrimethylammoniumbromide (Aldrich, Milwaukee, WI); 100-mm silicon

(20) Gavin, P. F.; Ewing, A. G. *Anal. Chem.* **1997**, *69*, 3838−3845.
(21) Woolley, A. T.; Lao, K.; Glazer, A. N.; Mathies, R. A. *Anal. Chem.* **1998**, *70*, 684−688.
(22) Martin, R. S.; Gawron, A. J.; Fogarty, B. A.; Regan, F. B.; Dempsey, E.; Lunte, S. M. *Analyst* **2001**, *126*, 277−280.
(23) Gawron, A. J.; Martin, R. S.; Lunte, S. M. *Electrophoresis* **2001**, *22*, 242−248.
(24) Martin, R. S.; Gawron, A. J.; Lunte, S. M.; Henry, C. S. *Anal. Chem.* **2000**, *72*, 3196−3202.
(25) Henry, C. S.; Zhong, M.; Lunte, S. M.; Moon, K.; Bau, H.; Santiago, J. J. *Anal. Commun.* **1999**, *36*, 305−308.
(26) Wang, J.; Chatrathi, M. P.; Ibanez, A. *Analyst* **2001**, *126*, 1203−1206.
(27) Wang, J.; Chatrathi, M. P.; Ibanez, A. *Anal. Chem.* **2001**, *73*, 1296−1300.
(28) Wang, J.; Chatrathi, M. P.; Tian, B. *Anal. Chem.* **2000**, *72*, 5774−5778.
(29) Wang, J.; Tian, B.; Sahlin, E. *Anal. Chem.* **1999**, *71*, 5436−5440.
(30) Rossier, J. S.; Ferrigno, R.; Girault, H. H. *J. Electroanal. Chem.* **2000**, *492*, 15−22.
(31) Chen, D.-C.; Hsu, F.-L.; Zhan, D.-Z.; Chen, C.-H. *Anal. Chem.* **2001**, *73*, 758−762.
(32) Hilmi, A.; Luong, J. H. T. *Anal. Chem.* **2000**, *72*, 4677−4682.
(33) Hilmi, A.; Luong, J. H. T. *Environ. Sci. Technol.* **2000**, *34*, 3046−3050.
(34) Schwarz, M. A.; Galliker, B.; Fluri, K.; Kappes, T.; Hauser, P. C. *Analyst* **2001**, *126*, 147−151.
(35) Liu, Y.; Fanguy, J. C.; Bledsoe, J. M.; Henry, C. S. *Anal. Chem* **2000**, *72*, 5939−5944.
(36) Culbertson, C. T.; Jacobson, S. C.; Ramsey, J. M. *Anal. Chem.* **2000**, *72*, 5814−5819.
(37) Burggraf, N.; Manz, A.; Verpoorte, E.; Effenhauser, C. S.; Widmer, H. M.; de Rooij, N. F. *Sens. Actuators, B* **1994**, *20*, 103−110.
(38) Becker, H.; Gartner, C. *Electrophoresis* **2000**, *21*, 12−26.
(39) Huang, X.; Zare, R. N.; Sloss, S.; Ewing, A. E. *Anal. Chem* **1991**, *63*, 189−192.

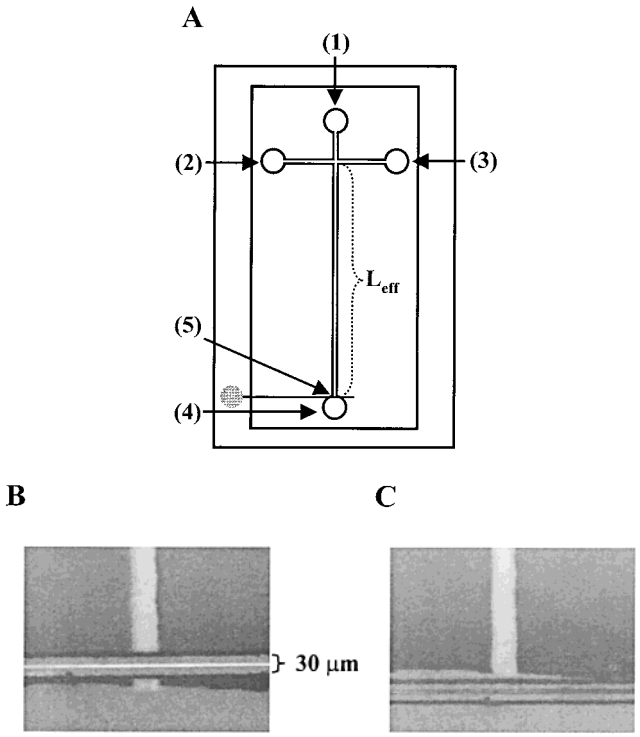

Figure 1. Chip layout and electrode alignments used in these studies: (A) chip layout (see text for dimensions); 1−4 represent fluid reservoirs, 5 represents relative location of working electrode; with unpinched injections, buffer is placed in reservoir 1 and sample is placed in reservoir 2, vice versa for gated injections; 3 and 4 correspond to the sample waste and detection reservoirs, respectively; effective separation length is denoted as L_{eff}; (B) in-channel alignment; and (C) end-channel alignment.

wafers (Silicon Inc., Boise, ID); 125-mm silicon wafers (MEMC Electronic Materials, Inc., St. Peters, MO); Sylgard 184 (Ellsworth Adhesives, Germantown, WI); carbon fibers (Avco Specialty Materials, Lowell, MA); boric acid, sodium cyanide, catechol, sodium nitrite, and glycine (Sigma, St. Louis, MO); naphthalene-2,3-dicarboxaldehyde (Molecular Probes, Eugene, OR); and colloidal silver (Ted Pella, Inc., Redding, CA).

Chip Designs. Poly(dimethylsiloxane) (PDMS)-based microfluidic devices with carbon fiber working electrodes were fabricated as previously described.[23] This procedure entailed the fabrication of two separate PDMS layers, one containing the separation and injection channels and one containing an electrode channel for the carbon fiber. Chip designs were of the standard type, with a simple T configuration and reservoirs for buffer, sample, sample waste, and detection electrodes (Figure 1A).[23,24] Three different chip designs were used in this work, with all channels being 35 μm in width and 30 μm in depth. Studies involving catechol were performed on a chip with an effective separation length (L_{eff}, distance from injection T to end of channel, see Figure 1A) of 35 mm, but studies with nitrite had an effective separation length of 54 mm and those involving cyanobenz[*f*]-isoindole (CBI)−glycine had an effective separation length of 43 mm.

Two different electrode alignments were used in these studies (Figure 1B,C). Both were accomplished by aligning the carbon fiber working electrode at the end of the separation channel with the aid of a light microscope and calibrated reticule. The in-channel arrangement (Figure 1B) was afforded by aligning and reversibly sealing the center of the 30-μm carbon fiber directly in the separation channel, 25 μm from the end. The end-channel arrangement (Figure 1C) was accomplished by aligning and reversibly sealing the center of the 30-μm carbon fiber outside the separation channel 25 μm from the end.

Electrophoresis Procedures. Stock solutions of catechol and sodium nitrite were prepared in water (1 and 10 mM, respectively). Appropriate dilutions were made with water prior to use. CBI−glycine was prepared by derivatizing glycine with naphthalene-2,3-dicarboxaldehyde in the presence of cyanide at pH 9.2, as previously described.[40] The derivatization reaction was performed so that the final buffer concentration was approximately equal to that of the separation buffer. The electrophoresis buffer for the studies involving catechol and CBI−glycine was 20 mM boric acid, pH 9.2. The analysis of nitrite was accomplished using a 15 mM boric acid buffer at pH 9, with 7.5 mM dodecyltrimethylammoniumbromide (DTAB) added as an EOF modifier. In all cases, filtered and degassed buffer was introduced into the reservoirs and flushed through the channels via vacuum prior to use.

Effective field strengths were calculated from the point of injection using Kirchhoff's rules.[41] Separations involving catechol and CBI−glycine were performed using a field strength of 300 V/cm, but the nitrite separation was accomplished using a field strength of 100 V/cm. Studies involving catechol were performed in triplicate and employed unpinched injections. This entailed applying a high voltage to the sample reservoir for 1 s with both the sample waste and detection reservoirs grounded and the buffer reservoir left floating (Figure 1A).[22−24,29,42] After the injection was complete, the separation voltage was applied to the buffer reservoir, and the separation was performed using a Spellman CZE 1000R high-voltage power supply (Spellman High Voltage Electronics, Hauppauge, NY) with the detection reservoir grounded. The analysis of nitrite was performed in a similar manner except that a negative polarity was used for both injection and separation. Studies involving CBI−glycine ($n = 5$) utilized a gated injection scheme,[43,44] which was performed using two Spellman high-voltage power supplies. A high voltage was applied to the buffer reservoir, and a fraction of that voltage (0.87) was applied to the sample reservoir with the sample waste and detection reservoirs remaining at ground (Figure 1A). Injections were made by floating the power supply that was connected to the buffer reservoir for a period of 1 s.

Electrochemical Detection with Electrically Isolated Potentiostat. The design of the electrically isolated potentiostat was based on a recent "system-on-a-chip" (SOC) innovation, the Cygnal 8051F000 (CYGNAL Integrated Products, Inc., Austin, TX), that, as shown in Figure 2, provides several components of a conventional 3-electrode digital potentiostat: analog-to-digital conversion (ADC), digital-to-analog conversion (DAC), voltage reference, timer, digital control, serial communication, and nonvolatile

(40) Nussbaum, M. A.; Przedwiecki, J. E.; Staerk, D. U.; Lunte, S. M.; Riley, C. M. *Anal. Chem.* **1992**, *64*, 1259−1263.
(41) Seiler, K.; Fan, Z. H.; Fluri, K.; Harrison, D. J. *Anal. Chem.* **1994**, *66*, 3485−3491.
(42) Wang, J.; Tian, B.; Sahlin, E. *Anal. Chem.* **1999**, *71*, 3901−3904.
(43) Jacobson, S. C.; Koutny, L. B.; Hergenroder, R.; Moore, A. W.; Ramsey, J. M. *Anal. Chem.* **1994**, *66*, 3472−3476.
(44) Jacboson, S. C.; Hergenroder, R.; Moore, A. W.; Ramsey, J. M. *Anal. Chem.* **1994**, *66*, 4127−4132.

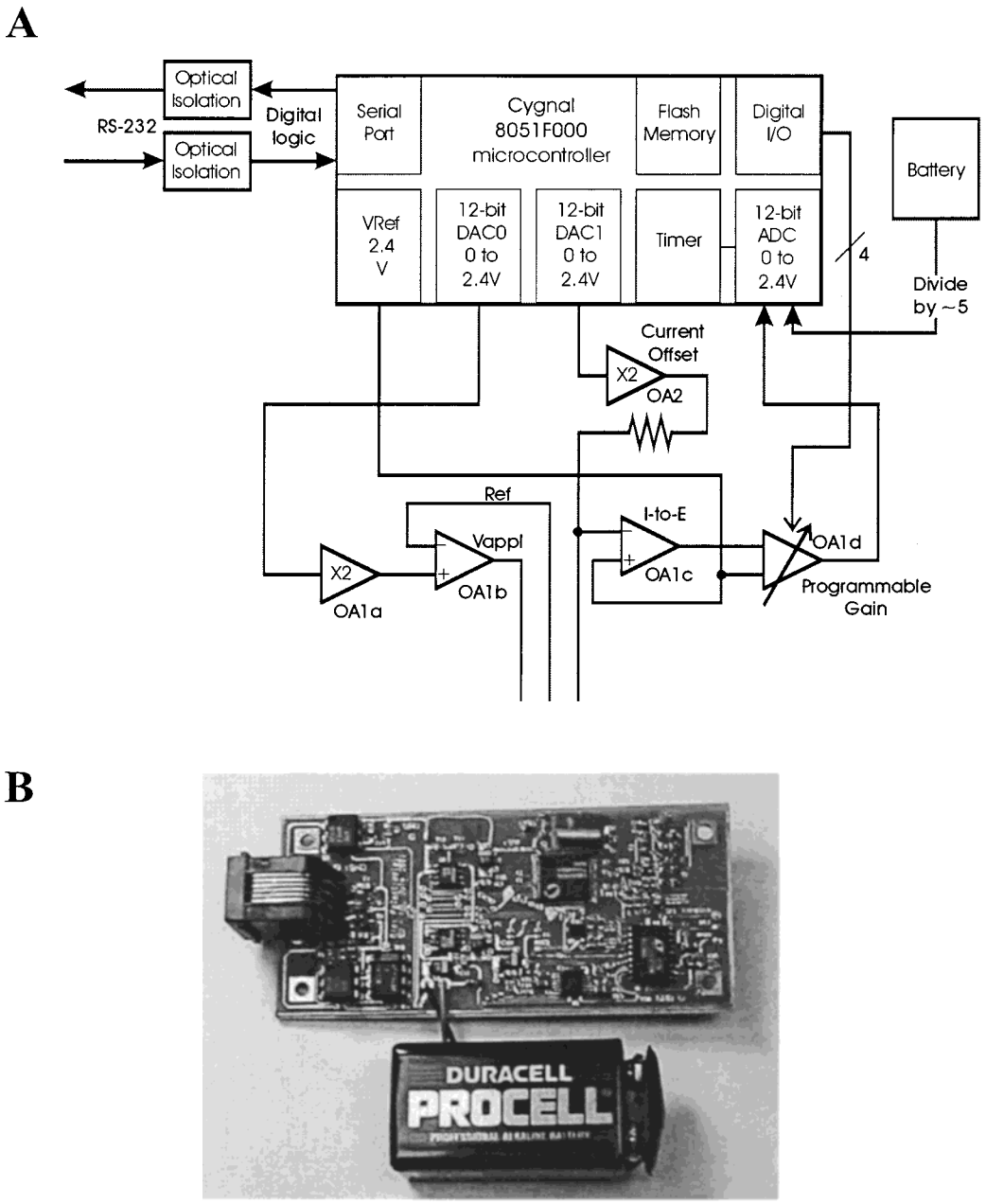

Figure 2. (A) Block diagram of the isolated potentiostat and (B) picture of the minipotentiostat with a 9 V battery.

memory. The host PC, communicating with the potentiostat over an electrically isolated RS-232 port, controls the overall experiment with simple ASCII-based commands, and the SOC system affects the hardware control and timing. Industry-standard H11L1 opto-isolators provide 7.5 kV isolation.

This SOC, like most new microprocessors, is a 3 V device; therefore, its analog input and output ranges must be less than that—in this case, 2.048 V. Consequently, amplification was needed to give the DACs the bipolar range required for electrochemical measurements. To accomplish this, OA1a (operational amplifier 1a, see Figure 2A) doubled the output of DAC0 before feeding the electrode amplifier, OA1b. The voltage reference was used to set a virtual ground near the midpoint of the doubled DAC output so that the generated applied voltage, V_{appl}, was in the range of −2 to +2.9 V with respect to the virtual ground. The current-to-voltage (*i*-to-*E*) converter, OA1c, was included in a quad operational amplifier (LT1053, Linear Technology Corporation, Milpitas, CA). Because of the need for a virtual ground, the programmable gain amplifier (PGA) integrated in the SOC could not be used, and a new PGA was constructed from an amplifier, OA1d, and an analog switch. The experiments described here required a stable offset current capability, which was generated from a DAC whose output was doubled (OA2) to match the voltage range of the system. At present, the draw on the 9 V battery is about 12 mA during data acquisition and as low as 4 mA at idle.

This current design was not optimized to minimize noise. The root-mean-square noise level, unshielded at ~50 Hz bandwidth, was ~70 pA. The system must also be calibrated before being placed in service. Using the SOC's flash memory, calibration parameters were stored on the SOC itself so that they remain with the instrument if it is used on more than one computer. The firmware was developed in assembly language and also stored in

flash memory. Operations include control of all peripherals, communication, signal averaging, and timing. The resulting electropherograms were saved to an ASCII format and imported into ChromGraph Report (version 9.06, Bioanalytical Systems, West Lafayette, IN) for data analysis.

Electrical connection to the carbon fiber working electrode was made via copper wire and colloidal silver.[23] Other pertinent electrodes were reproducibly placed in the detection reservoir using a homemade Plexiglas holder with the reference electrode (Ag/AgCl, RE-6, Bioanalytical Systems) being positioned as close as possible to the end of the separation channel. This holder also contained the auxiliary and grounding electrodes, which were made from platinum wire.

LIF Detection. The LIF detection system that was used was similar to that described by Ocvirk et al.[19] Excitation light (442 nm) from a 32 mW HeCd laser (model IK5351R-D, Kimmon Electric US, Englewood, CO) was directed through a band-pass filter (442df10, Omega Optical, Brattleboro, VT) and into a dichroic filter (475DCLP, Omega Optical). The dichroic filter reflected the beam 90° into a long working distance microscope objective with correction cap (40X, LWD Plan Fluorite LCPLFL, Olympus America, Melville, NY). Using the objective, the laser beam was focused onto the microchip CE separation channel as a circular spot with a diameter of ~35 μm, ~300 μm from the in-channel carbon fiber working electrode (Figure 1B), and the fluorescence was collected with the same objective. The collected fluorescence was passed through the dichroic filter and was refocused using an achromatic tube lens (f = 100 mm, PAC 052, Newport, Irvine, CA) into a photomultiplier tube (R1477, Hamamatsu, Bridgewater, NJ). The photomultiplier tube was encased in a tube housing (70680, Thermo Oriel, Stratford, CT) and operated at a voltage of +1000 V, which was supplied by a regulated power supply (model 227, Pacific Photometric, Concord, CA). The signal was amplified using a low-noise preamplifier (model SR570, Stanford Research System, Sunnyvale, CA), and data was collected using a DA-5 analog-digital converter (Bioanalytical Systems) that was interfaced to a Dell personal computer. Data analysis was performed using ChromGraph Report (version 9.06, Bioanalytical Systems).

RESULTS AND DISCUSSION

Electrode Alignment and Electrically Isolated Potentiostat. The PDMS-based devices used in this work utilized carbon fiber working electrodes. Previous work in our laboratory[23] has shown that these EC detectors are stable and robust, in contrast to devices that utilize metal film electrodes, which often suffer from electrode instability upon exposure an electric field.[10,24] Most reported microchip CEEC devices have used some variant of an end-channel alignment scheme similar to that shown in Figure 1C.[21−29,33−35] This type of alignment leaves a small gap (in this case, 10 μm) between the front of the working electrode and the end of the separation channel. This approach provides sufficient grounding of the separation voltage through the cathode so that conventional potentiostats, which are also tied to ground, can be used to monitor the separation.

The development of the electrically isolated potentiostat (see Experimental Section and Figure 2) enables the working electrode to be placed directly in the separation channel (Figure 1B). The floating potentiostat was designed using digital communication with an on-board microcontroller that controls all analog signal processing. This helps to simplify electrical isolation and results in a compact (4 × 9 × 2 cm, see Figure 2B), low-power system. Since data are transmitted over an electrically isolated RS-232 port, the detection circuitry does not provide a path to ground. This permits placement of the working electrode directly in the separation channel, without the need for a decoupling mechanism, and significantly simplifies the microchip design. This in-channel configuration should help to eliminate some of the negative separation performance characteristics encountered with an end-channel configuration that are due to the gap between the working electrode and the end of the separation channel (discussed below). Additionally, this in-channel configuration should not generate any backpressure, which can lead to band dispersion phenomena that are sometimes found in decoupled systems.[45] This enables a direct comparison between in-channel and end-channel alignments for EC detection.

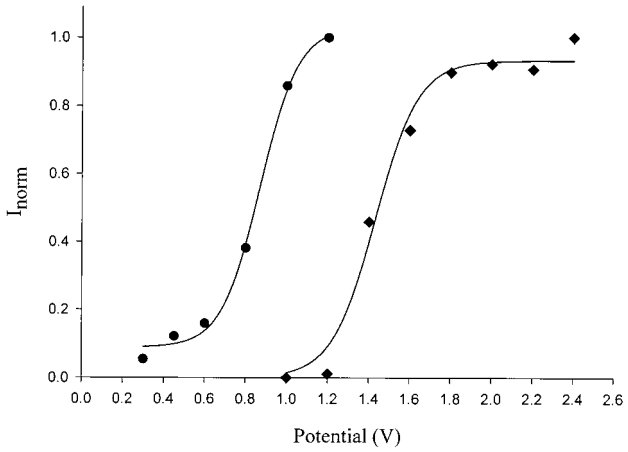

Figure 3. HDVs recorded for catechol using in-channel (◆) and end-channel (●) EC detection. Conditions: 20 mM boric acid buffer, pH 9.2, E_{sep} = 300 V/cm, potentials vs a Ag/AgCl reference.

Shift in Half-Wave Potential. Previous studies with conventional CEEC have shown that, in contrast to decoupled systems, an end-column detection scheme (similar to that described here) leads to positive shifts in the half-wave potentials of oxidizable compounds.[46] It was found that this shift occurs as a function of both the separation voltage and the distance of the electrode from the end of the fused-silica capillary.[46] A similar study was performed here with hydrodynamic voltammograms (HDVs) of catechol being generated for both end-channel and in-channel EC detection. As shown in Figure 3, the half-wave potential for catechol was shifted +600 mV as the working electrode was moved from an end-channel alignment to an in-channel alignment. This shift is consistent with the effect seen in conventional end-column CEEC.[46] For the simple amperometric detection scheme described here, this shift should not pose a significant problem, since a large detection potential can be applied to compensate for the shift. The shift does need to be taken into account when determining optimum applied potentials for EC detection so that the maximum response is obtained. Therefore, to ensure that the optimum potential is chosen, an HDV should be run for each analyte of interest.

(45) Wallingford, R. A.; Ewing, A. G. *Anal. Chem.* **1987**, *59*, 1762−1766.
(46) Wallenborg, S. R.; Nyholm, L.; Lunte, C. E. *Anal. Chem.* **1999**, *71*, 544−549.

In-Channel vs End-Channel EC Detection. Calculations of plate height and peak symmetry (as peak skew) were used to compare the performances of the two alignment schemes depicted in Figure 1. The significant contributions to total plate height (H_{tot}) in a microchip CE system are

$$H_{tot} = H_{inj} + H_{det} + H_{diff} + H_{ads} \quad (1)$$

where H_{inj} is from the injection plug length, H_{det} is from the detector observation length, H_{diff} is from axial diffusion, and H_{ads} is from analyte adsorption.[47]

As mentioned previously, end-channel EC detection is accomplished by aligning the working electrode tens of microns from the end of the separation channel. The distance between the working electrode and the end of the separation channel undoubtedly leads to some peak dispersion. Furthermore, peaks originating from microchip CEEC with end-channel detection are often unsymmetrical and exhibit tailing. This may be due to the fact that, with an end-channel alignment, the analyte bands exit the separation channel and are swept into a comparatively large detection reservoir before they migrate toward the working electrode to be detected. This migration is determined by the effective field strength and the electroosmotic flow generated in the separation channel, and it has previously been shown that potential fields dramatically decrease at the end of a capillary.[48] In addition to migrating in the direction of the working electrode, analytes may begin to disperse throughout the detection reservoir in multiple directions. This includes across and down the surface of the working electrode, because there is no active mechanism to sweep them entirely away.

The total exposed surface area of the working electrode in the detection reservoir is also fairly large, as compared to the size of the analyte band that elutes from the separation channel (Figure 1C). With an in-channel alignment, the exposed surface area of the working electrode is much smaller (in this case, $35 \times 30\ \mu$m, Figure 1B), and since the working electrode is placed in the separation channel, analytes are forcibly swept past the electrode surface; thus, none of the dispersion or diffusion that can take place with an end-channel alignment is allowed to occur. Therefore, the plate height term originating from the EC detector (H_{EC-det}) can be described by

$$H_{EC-det} = H_{electrode-size} + H_{electrode-alignment} \quad (2)$$

where $H_{electrode-size}$ correlates to the active surface area of the working electrode, and $H_{electrode-alignment}$ is related to any peak dispersion arising from the alignment of the working electrode. Since all of the experimental parameters except electrode alignment were kept constant in these studies, the contributions of H_{inj}, H_{diff}, and H_{ads} to H_{tot} are constant, and any change in H_{tot} should reflect only the contribution of H_{EC-det}.

Another measure of separation performance is peak symmetry. The symmetry of a peak is frequently measured by calculating the amount of peak skew. The data analysis software used in this work measures the peak skew using a formula that divides the peak in half at its apex and calculates the amount of skew by

$$\text{skew} = \frac{\text{area after apex} \times 2}{\text{area before apex} + \text{area after apex}} \quad (3)$$

so that perfect symmetrical peaks have a value of 1.0, but tailing peaks have a value greater than 1.0.

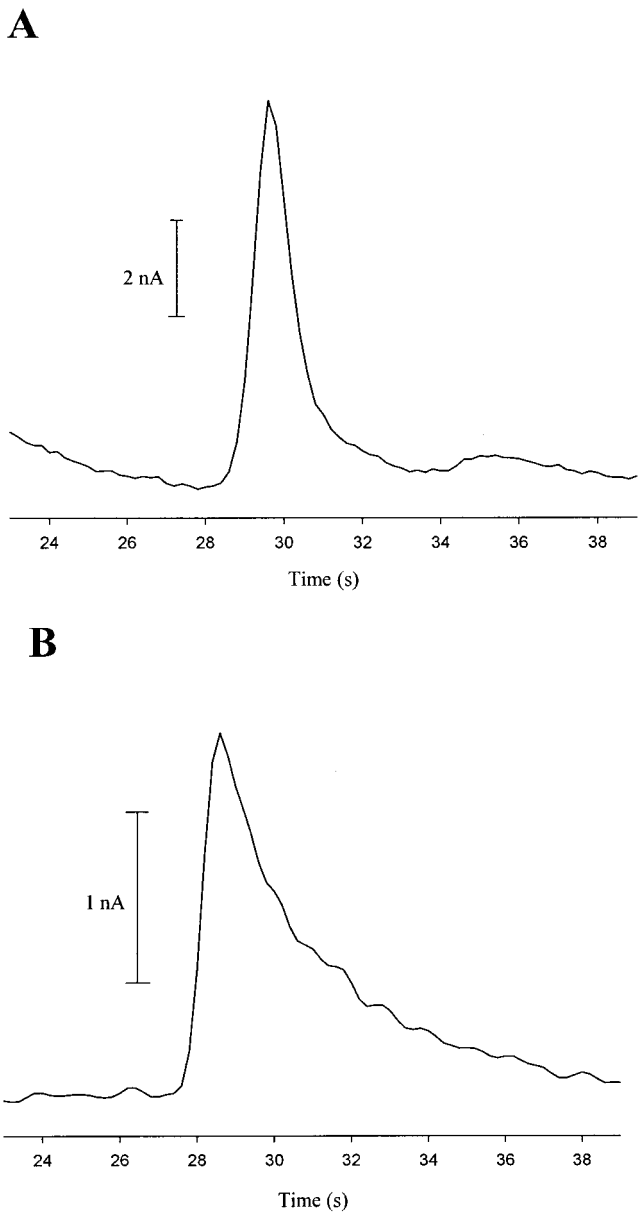

Figure 4. Electropherograms for catechol using (A) in-channel EC detection at +2.2 V and (B) end-channel EC detection at +1.0 V. Conditions same as in Figure 3.

Two electrochemically active analytes, catechol and nitrite, were used to compare the separation performance of in-channel and end-channel EC detection. As can be seen in Figure 4 and Table 1, in-channel EC detection of catechol results in more efficient, less skewed peaks than are seen with end-channel alignment. The use of the in-channel alignment results in a 4.6-fold decrease in H_{tot} and a 1.3-fold decrease in peak skew. Figure 4 clearly shows the increased performance achieved by the in-channel approach. The limits of detection for catechol using both

(47) Jacobson, S. C.; Hergenroder, R.; Koutny, L. B.; Ramsey, J. M. *Anal. Chem.* **1994**, *66*, 2369−2373.
(48) Sloss, S.; Ewing, A. G. *Anal. Chem.* **1993**, *65*, 577−581.

Table 1. Comparison of In-Channel and End-Channel EC Detection of Catechol and Nitrite

	separation length (mm)	N	H (μm)	skew
in-channel EC, catechol	35	4880	7.2	1.20
end-channel EC, catechol	35	1065	32.9	1.61
in-channel EC, nitrite	54	14520	3.7	0.93
end-channel EC, nitrite	54	11630	4.6	1.20

Table 2. Comparison of In-Channel EC and LIF Detection of CBI−Glycine

	separation length (mm)	N	H (μm)	skew
in-channel EC	43	7680	5.6	1.06
LIF	43	7800	5.5	0.88

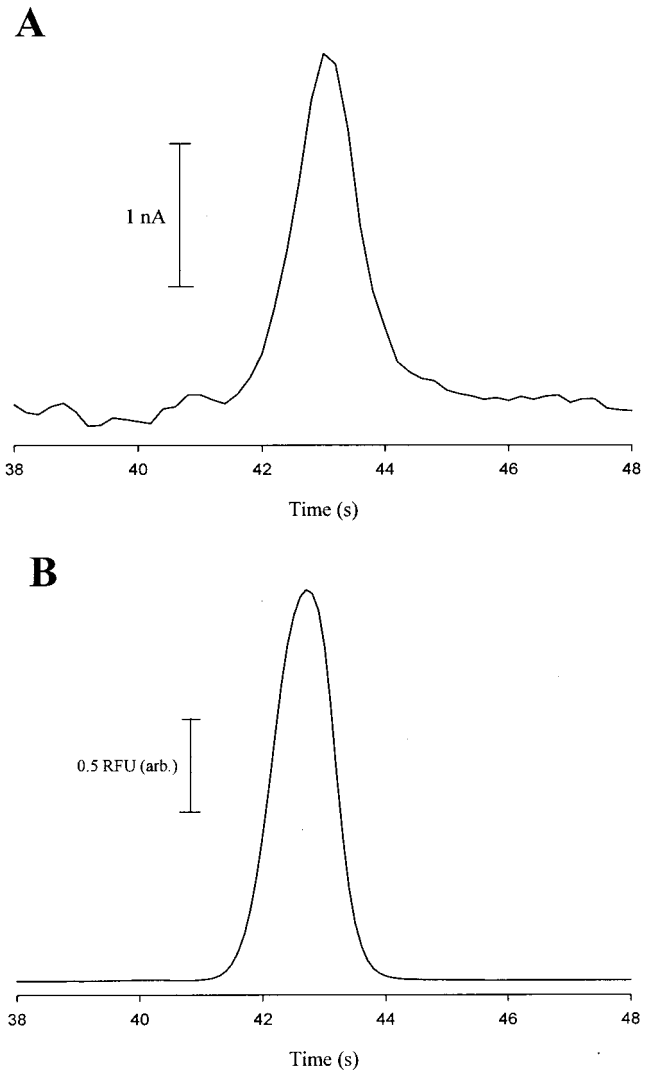

Figure 5. Electropherograms for CBI−Gly using (A) in-channel EC detection at +2.4 V and (B) LIF detection. Conditions same as in Figure 3.

alignments were ~4 μM at a S/N of 3. It is believed that the limits of detection can be substantially improved by lowering the background noise of the potentiostat with shielding; further layout improvements; application of noise-reduction algorithms; and new low-noise, low-voltage amplifiers. Fabricating the reference electrode in an equilateral position with respect to the working electrode should also help to lower the background noise.[49] All of these modifications are currently being investigated.

To further compare the performance of the two electrode configurations, the small, non-PDMS-adsorbing ion nitrite was analyzed under reversed electroosmotic flow conditions using DTAB as a flow modifier. As shown in Table 1, the in-channel alignment scheme also shows increased performance with this analyte. The use of the in-channel alignment decreased the total plate height by a factor of 1.2 and lowered the peak skew by a factor of 1.3. These findings and the results from the catechol experiments demonstrate that an in-channel detection scheme offers increased separation performance in terms of plate height and peak symmetry. The contribution of H_{EC-det} to H_{tot} is significantly reduced when the surface area of the working electrode is confined to the cross-sectional area of the separation channel and there is no gap between the end of the separation channel and the working electrode (in-channel EC detection).

In-Channel EC Detection versus LIF Detection. To compare in-channel EC detection with the popular LIF detection scheme, a fluorescent and electrochemically active analyte was used.[40] As seen in Figure 5 and Table 2, the separation performances of both detection schemes are very similar both in terms of plate height and peak skew. The number of theoretical plates obtained with LIF detection was comparable to that reported by others using PDMS devices with fluorescein-based dyes.[50] Since all the conditions were kept constant for the EC and LIF experiments and the detector observation lengths are approximately equal (laser beam spot, ~35 μm in diameter; active electrode surface area, 30 × 35 μm), it can be concluded that the plate heights for both detection schemes are essentially equal, and with these PDMS-based devices, the separation performance of in-channel EC detection is equivalent to LIF detection.

CONCLUSIONS

A new electrode configuration for microchip CE with EC detection has been described. This in-channel alignment scheme does not require the use of a decoupler and was made possible by the development of a novel, electrically isolated potentiostat. It was shown that aligning the electrode directly in the separation channel leads to a vast improvement in the performance of EC detection for microchip CE compared to the commonly used end-channel alignment. Furthermore, studies comparing in-channel EC and LIF detection showed that they exhibited similar separation performances in terms of plate height and peak symmetry. The approach described here should help to promote more widespread acceptance of electrochemistry as a detection mode for microchip CE.

The goal of the initial development of this prototype minipotentiostat was to gauge the separation performance of the in-channel alignment, not to minimize noise and compare limits of detection. Future work will focus on improving the minipotentiostat design to lower the background noise and, as a result,

(49) Klett, O.; Bjorefors, F.; Nyholm, L. *Anal. Chem.* **2001**, *73*, 1909−1915.

(50) Zhang, C.; Manz, A. *Anal. Chem.* **2001**, *73*, 2656−2662.

decrease the limits of detection. Future studies will also continue to evaluate the in-channel detection scheme by characterizing the separation performance of various analytes as a function of their native electrophoretic mobilities and the bulk electroosmotic flow, performing similar comparisons to LIF detection in microchip devices fabricated from other materials, such as glass and various plastics, and incorporating miniature USB-based power supplies[23] along with this minipotentiostat to develop a hand-held separation-based sensor.

ACKNOWLEDGMENT

The authors thank Dr. Ruri Kikura-Hanjiri (former visiting scientist at the University of Kansas, currently at the National Institute of Health Sciences, Tokyo, Japan) for her assistance in the nitrite analysis, John Ledford (Instrumentation Design Laboratory) for laying out the PC board, and Juan Hernandez (Instrumentation Design Laboratory) for assembling it. This research was supported by a grant from the National Science Foundation (CHE-9702631) and a postdoctoral fellowship (R.S.M.) from the National Institutes of Health. We also thank Nancy Harmony for her assistance in the preparation of this manuscript and Marlin Harmony for helpful discussions in constructing the LIF detection system.

Received for review October 12, 2001. Accepted November 28, 2001.

AC011087P